Experimental and theoretical studies on the structure and spectroscopic properties of (E)-1-(2-aminophenyl)-3-(pyridine-4-yl)prop-2-en-1-one

Andrés Felipe Cruz Ortiz [a, b], Alberto Sánchez López [a, *], Alejandro García Ríos [a], Fernando Cuenú Cabezas [b], Ciro Eduardo Rozo Correa [c]

[a] Grupo de Investigación en Fisicoquímica Ambiental y Computacional, Programa de Química, Universidad Del Quindío, Carrera 15, Calle 12 Norte, Armenia, Colombia
[b] Laboratorio de Química Inorgánica y Catálisis, Programa de Química, Universidad Del Quindío, Carrera 15, Calle 12 Norte, Armenia, Colombia
[c] Grupo de Investigaciones Ambientales Para el Desarrollo Sostenible, Facultad de Química Ambiental, Universidad Santo Tomas, Floridablanca, Colombia

ARTICLE INFO

ABSTRACT

(E)-1-(2-aminophenyl)-3-(pyridine-4-yl)prop-2-en-1-one (or simply 2-aminochalcone) was synthetized and characterized by elemental analysis, FT-IR, NMR, MS and XRD. Molecular geometry optimization, vibrational harmonic frequencies, ^1H and ^{13}C NMR chemical shifts were calculated by ab initio (HF and MP2) and density functional theory (DFT) methods, with B3LYP and B3PW91 functionals, using GAUSSIAN 09 program package without any constraint on the geometry. With VEDA software vibrational frequencies were assigned in terms of the potential energy distribution. A detailed interpretation of the FT-IR, NMR and XRD, experimental and calculated, is reported. The HOMO and LUMO energy gap that reflects the chemical activity of the molecule were also studied by DFT and above basis set. All theoretical results correspond to a great extent to experimental ones.

1. Introduction

Chalcones are flavonoid type organic compounds [1] that can be obtained from natural products or organic synthesis, via aldol condensation. The name chalcone was given by Kostanecki and Tambor [2]. It is formed by two aromatic rings linked by three carbon atoms that form an unsaturated α, β system, which is a key factor in the synthesis of compounds such as benzothiazepines [3], pyrazoline [4], 1,4-diketone [5], flavones [6] and other biologically important heterocycles with pharmacological important properties, e.g. antitumor agents [7], antioxidants [8], anti-inflammatory [9] and antifungal [10]. Its excellent optical properties that include high extinction coefficients for UV absorption and significant nonlinear optical responses [11–13], lead to potential applications in new drugs and agrochemicals design [14]. Moreover, some of the chalcones derivatives have shown excellent properties to inhibit important enzymes in cellular systems, such as xanthine oxidase [15] and tyrosine kinase [16,17].

Chalcone type compounds have been studied at the ab initio and DFT levels of theory, to analyze their geometry, normal vibrational modes, ^1H and ^{13}C NMR chemical shifts, in order to perform a painstaking structural characterization and thus verify experimental data [18–20].

In this work, 2-aminochalcone (Fig. 1) molecular geometry, spectroscopic and electronic properties were studied at levels of ab initio and DFT, with 6–311++G (d,p) basis set. In all cases, molecular structure was optimized to be the lower energy structure and hence the more stable in agreement with experiment, followed by a vibrational frequencies calculation at the optimized geometry, the stability of wave function was verified, ^1H and ^{13}C NMR chemical shifts and HOMO and LUMO energy gap was obtained.

2. Experimental details

2.1. 2-Aminochalcone synthesis

The synthesis was performed following the methods reported in literature [21]. A mixture of 2-aminoacetophenone (2.8 mmol),

* Corresponding author. Carrera 15 Calle 12 N, Armenia, Quindío, Colombia.
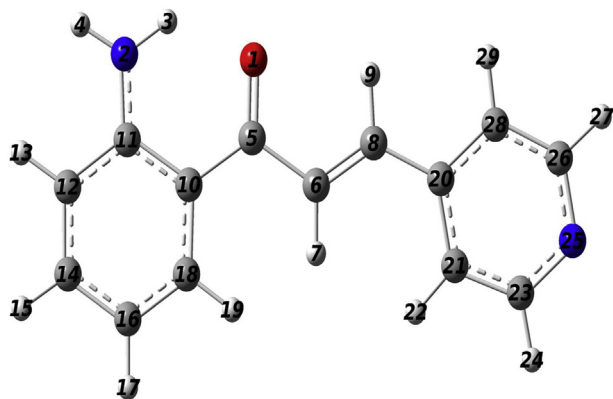E-mail address: gifac@uniquindio.edu.co (A. Sánchez López).

Fig. 1. Numbering Scheme 2-aminochalcone.

pyridine-4-carbaldehyde (2.8 mmol), ethanol (10 mL) and 20% aqueous sodium hydroxide solution (0.5 mL) was heated under reflux for 20 min (Scheme 1). The mixture was cooled to ambient temperature, and the resulting solid was collected by filtration, then successively washed with ethanol (2×0.5 mL) and water (2×0.5 mL), finally it was dried at reduced pressure. The result was an orange solid (yield 84%, mp 166–167 °C) that was characterized by elemental analysis, FT-IR, MS, XRD, ^{1}H and ^{13}C NMR. Elemental analyses were carried out on a CHN Analyzer Flash EA 1112 Series. FT-IR spectrum was recorded with a Thermo Nicolet 320 FT-IR Spectrophotometer, through KBr pellet dispersion method. Mass spectrum (70 eV) was performed in a GC/MS-QP2010 mass spectrometer. ^{1}H and ^{13}C NMR were carried out in a Bruker Avance 400 spectrophotometer, using DMSO-d_6 as solvent and the chemical shifts are reported relative to tetramethylsilane (chemical shifts in δ values, J in Hz). The structures of 2-aminochalcone compound was deduced from the results of ^{1}H and ^{13}C NMR. FT-IR in KBr Pellet (Fig. 2), showed characteristic bands at ν_{max} (cm^{-1}): 3392, 3263, 1621 (amine group N—H), 3139, 3077 (phenylamine ring C═C—H), 3029 (pyridine ring C═C—H), 1648, 650 (system α, β-unsaturated C═O), 1585 (pyridine ring C═N), 1546 (pyridine ring C═C), 1481, 1415 (phenylamine ring C═C). Assignments of NMR chemical shifts were performed according to the 2-aminochalcone numbering scheme (Fig. 1). ^{1}H NMR —(400 MHz, DMSO-d_6 (Fig. 3))—, δ (ppm): 8.64 (d, 2H, J 5.5 Hz, H(27)), 8. 18 (d, 1H, J 15.6 Hz, H(7)); a 8.09 (d, 1H, J 8.04 Hz, H(19)), 7.80 (d, 2H, J 5.6 Hz, H(29)), 7.56 (d, 1H, J 15.6 Hz, H(9)), 7.48 (s, 2H, N—H of group amino) 7.30 (t, 1H, H(15)), 6.81 (d, 1H, H(13)), 6.59 (t, 1H, H(17)). ^{13}C NMR —(400 MHz, DMSO-d_6 (Fig. 4))—, δ (ppm): 190C(5), 152C(20), 150C(26), 142C(11), 139C(8), 135C(14), 132C(18), 128C(6), 122C(28), 118C (10), 117C(12), 115C(17). The elemental analyses for $C_{14}H_{12}N_2O$ (C 75.02%; H 5.37%; N 12.53%) is in a good agreement with the proposed composition (C 74.98%; H 5.39%; N 12.49%) which is further confirmed by MS: (70 eV) m/z (%) 224 (23.25, M^+), 146 (100, M-C_5H_4N), 120 (14.51, $C_8H_8N^+$), 92 (11.16, $C_6H_6N^+$) (Fig. 5).

3. Computational details

2-Aminochalcone crystallographic data [22] was used as a parameter for geometry optimization with methods ab initio (HF and MP2) and DFT (B3LYP and B3PW91), with the 6-311G++(d, p) basis set [23,24]. Optimized structural parameters were used to work out analytical vibrational frequencies, ^{1}H and ^{13}C NMR chemical shifts and HOMO and LUMO energy gap calculations. All quantum chemical calculations were performed with GAUSSIAN 09 [25] program package. With GAUSSVIEW 5.0.8 [26] molecular visualization software assistance vibrational frequencies were assigned. In addition, they were analyzed in terms of potential energy distribution with VEDA software [27].

4. Results and discussion

The elemental analysis and mass spectrometry of 2-aminochalcone (Fig. 1) are consistent with the molecular formula chalcone $C_{14}H_{12}N_2O$. It was characterized by FT-IR, ^{1}H and ^{13}C NMR instrumental techniques.

4.1. Structural analysis

Non-restricted optimized geometries for 2-aminochalcone were obtained from X-ray diffraction data [22]. Ab initio and DFT, with 6–311++G (d,p) basis set, calculations were done. Comparison between optimized structural and experimental parameters, according to numbering scheme (Fig. 1), is shown in Table 1.

Most of calculated bond lengths are slightly longer than the experimental values observed. According to crystallographic data [22], experimental C—C bond length can be observed between 1.473 Å–1.299 Å, calculated ones were between 1.498 Å–1.325 Å (HF), 1.492 Å–1.352 Å (MP2); 1.491 Å–1.343 Å (B3LYP); 1.486 Å–1.342 Å (B3PW91). Experimental C—H bond length are seen between 0.935 Å–0.929 Å and calculated ones were among 1.076 Å–1.072 Å (HF); 1.090 Å–1.086 Å (MP2); 1.087 Å–1.081 Å (B3LYP); 1.088 Å–1.082 Å (B3PW91). Experimental C—N bond length are observed between 1.332 Å–1.306 Å, calculated ones were detected at 1.367 Å–1.317 Å (HF); 1.384 Å–1.345 Å (MP2); 1.358 Å–1.335 Å (B3LYP); 1.353 Å–1.332 Å (B3PW91). Experimental N—H bond length are between 0.880 Å–0.879 Å, calculated ones were identified in 0.993 Å (HF); 1.012 Å–1.010 Å (MP2); 1.013 Å–1.005 Å (B3LYP); 1.014 Å–1.005 Å (B3PW91). The major differences from calculated structural parameter regarding experimental ones correspond to the C—H's bonds.

The greatest differences in calculated bond angles regarding experimental ones were 5.406° (HF) and 6.894° (MP2) for bond H(4)-N(2)-C(11). This is consistent with a molecule's geometric distortion where hydrogen from amino group is in a different plane to the aromatic ring. In addition, there is an intramolecular hydrogen bond that impact on the overall molecular conformation. In DFT methods the greatest differences were 2.401° (B3LYP) and
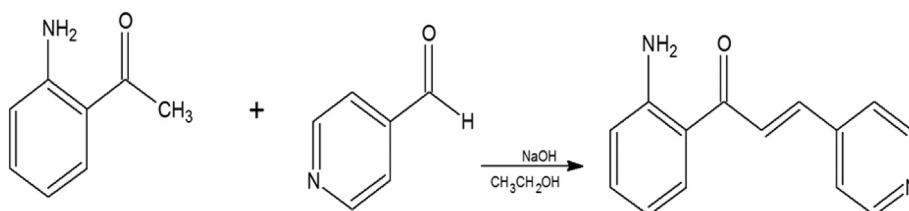
Scheme 1. Synthesis of 2-aminochalcone.
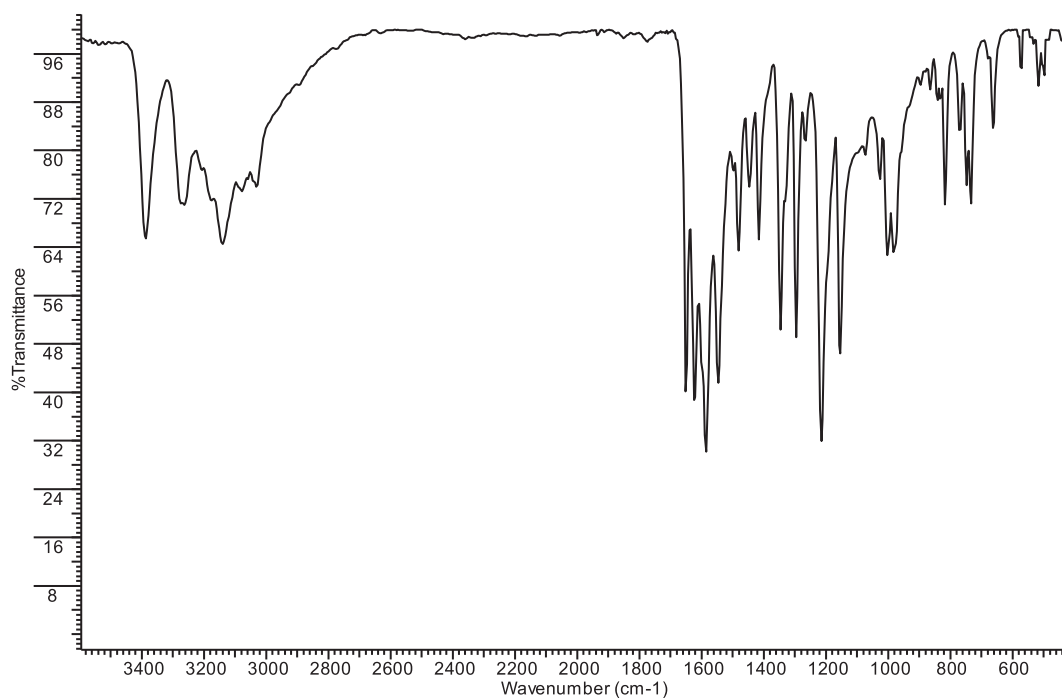
Fig. 2. Experimental FT-IR spectrum (in KBr Pellet) of 2-aminochalcone.
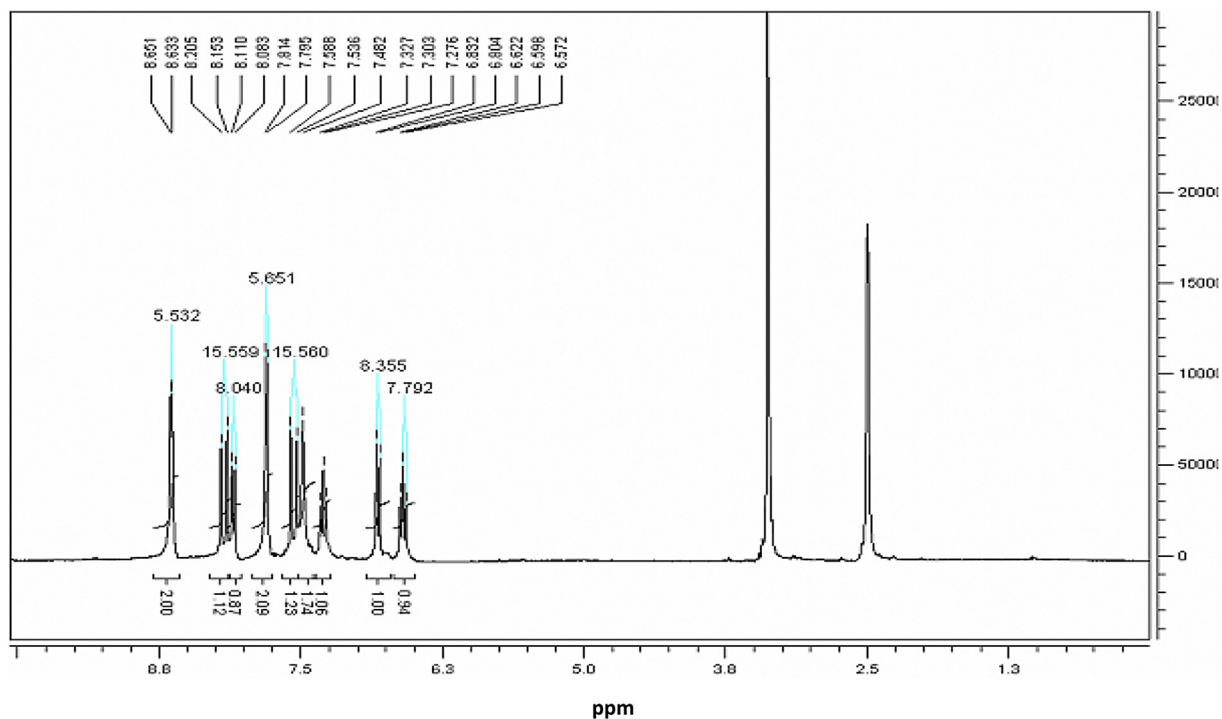
Fig. 3. Experimental ^{1}H NMR spectrum of 2-aminochalcone in DMSO-d6.

2.354° (B3PW91) in the angle C (21)-C (23)-H (24) from pyridine ring.

DFT level calculated 2-aminochalcone bond lengths and angles are closer to the experimental values due to, possibly, the presence of the electron correlation including the B3LYP and B3PW91 functional. Comparison of the calculated and experimental dihedral angles, according to the numbering scheme of Fig. 1, are presented

in Table 2. It was observed that the largest difference in calculated angles considering experimental ones was presented with the ab initio methods (HF and MP2), which is consistent with a distortion in the optimized geometry amino group with respect to the initial geometry. Similarly the DFT level calculated dihedral angles differ by no more than 3.6.

Calculated geometrical parameters represent a good
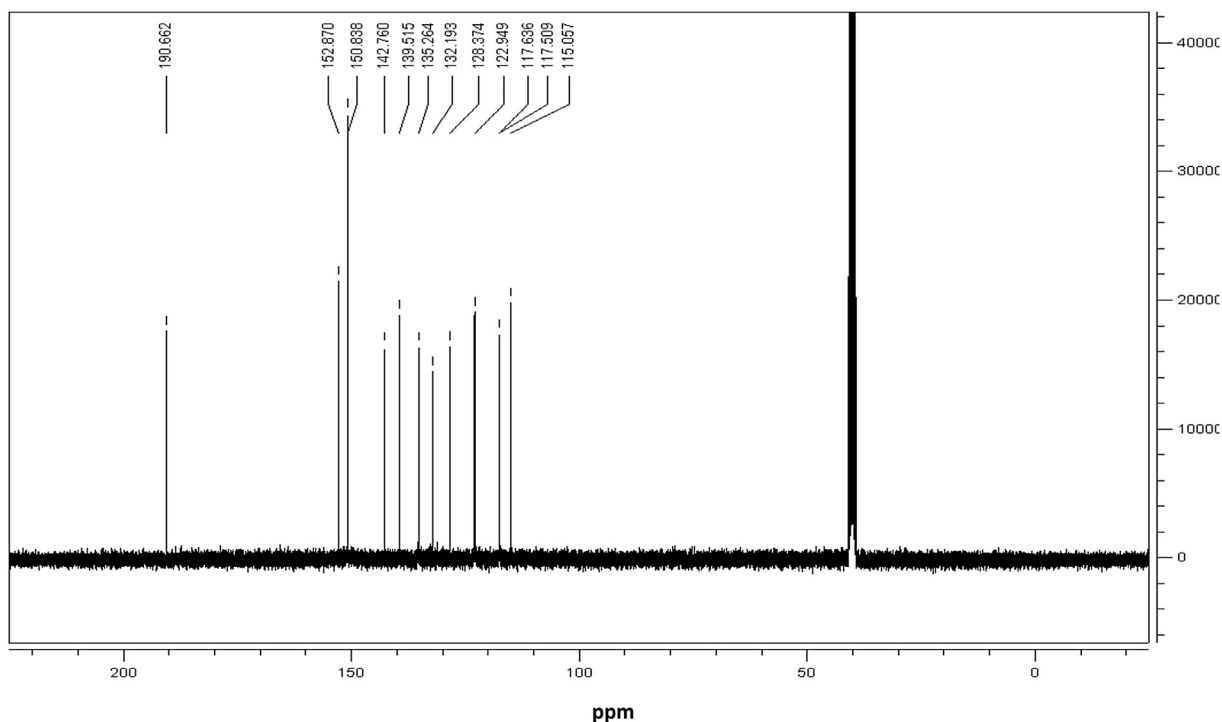
Fig. 4. Experimental ^{13}C NMR spectrum of 2-aminochalcone in DMSO-$d6$.
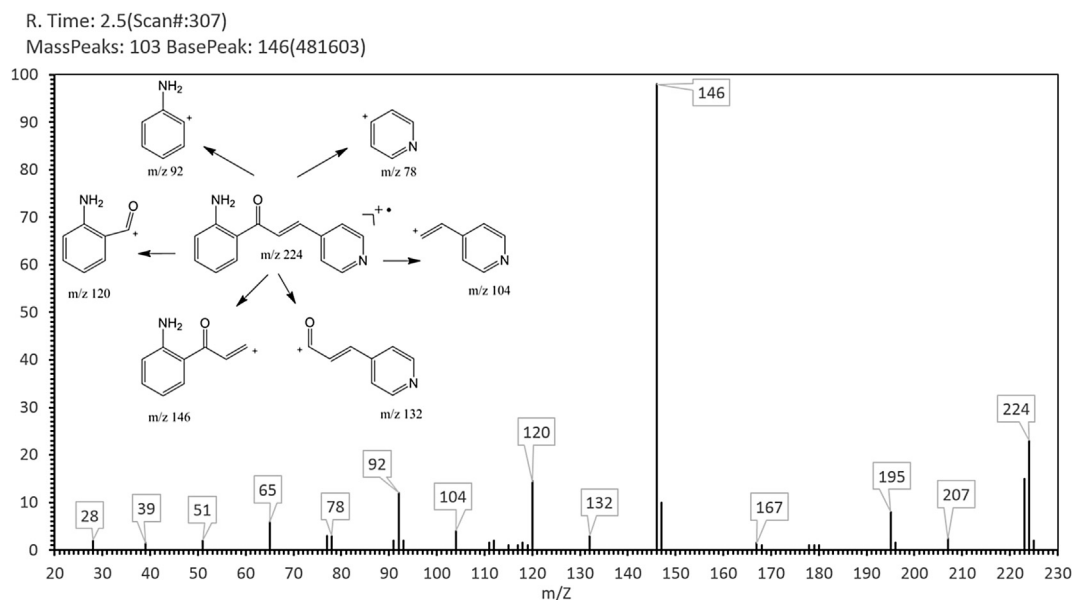
Fig. 5. Experimental mass spectrum (70 eV) of 2-aminochalcone.

approximation and can be used as the basis to calculate other parameters, such as vibrational frequencies, chemical shifts, and Fukui local reactivity indexes.

4.2. Vibrational analysis

Analytical vibrational frequencies for 2-aminochalcone were calculated from optimized geometries. The lack of imaginary frequencies inferred that optimization is in a minimum of the potential energy surface. Molecular conformation obtained by optimizing the geometry exhibits no spatial symmetry and, therefore, the molecule belongs to C_1 point group. According to 3N-6 formula, the molecule presents 81 normal modes of vibration. The assignments of the vibrational frequencies were done through GAUSSVIEW 5.0.8 software. Table 3 gives calculated and experimental vibrational frequencies. FT-IR experimental spectrum is shown in Fig. 2 and the calculated ones in Figs. 6–9. The discrepancies between calculated and experimental vibrational frequencies are due to two fundamental reasons: firstly, the experimental frequencies correspond to the solid phase (KBr pellet)

Table 1
Optimized geometrical parameters for 2-aminochalcone molecule computed at HF, MP2, B3LYP and B3PW91 with 6−311++G (d,p) basis set.

Bond length (Å)	Exp[a]	Ab initio		DFT		Bond angles (°)	Exp[a]	Ab initio		DFT	
		HF	MP2	B3LYP	B3PW91			HF	MP2	B3LYP	B3PW91
C(5)-O(1)	1.224	1.201	1.236	1.238	1.236	H(3)-N(2)-H(4)	120.77	116.46	115.14	121.26	121.68
N(2)-H(3)	0.879	0.993	1.012	1.013	1.014	H(3)-N(2)-C(11)	117.04	117.48	114.88	118.22	117.85
N(2)-H(4)	0.880	0.993	1.010	1.005	1.005	H(4)-N(2)-C(11)	122.18	116.77	115.28	119.81	119.96
N(2)-C(11)	1.332	1.367	1.384	1.358	1.353	O(1)-C(5)-C(6)	117.35	119.41	120.18	118.68	118.70
C(5)-C(6)	1.473	1.498	1.492	1.491	1.486	O(1)-C(5)-C(10)	121.85	121.95	122.21	121.64	121.74
C(5)-C(10)	1.452	1.486	1.484	1.477	1.472	C(6)-C(5)-C(10)	120.79	118.64	117.60	119.68	119.56
C(6)-H(7)	0.930	1.072	1.086	1.081	1.082	C(5)-C(6)-H(7)	119.32	118.63	118.78	119.26	119.41
C(6)-C(8)	1.299	1.325	1.352	1.343	1.342	C(5)-C(6)-C(8)	121.44	120.14	120.24	120.32	120.12
C(8)-H(9)	0.935	1.076	1.090	1.087	1.088	H(7)-C(6)-C(8)	119.24	121.22	120.96	120.41	120.46
C(8)-C(20)	1.451	1.477	1.466	1.464	1.461	C(6)-C(8)-H(9)	115.96	117.80	117.54	116.81	116.71
C(10)-C(11)	1.409	1.411	1.422	1.434	1.431	C(6)-C(8)-C(20)	128.02	126.24	125.16	127.08	126.95
C(10)-C(18)	1.392	1.401	1.412	1.413	1.410	H(9)-C(8)-C(20)	116.02	115.96	117.26	116.11	116.34
C(11)-C(12)	1.395	1.404	1.411	1.415	1.413	C(5)-C(10)-C(11)	120.95	121.02	120.96	120.39	120.29
C(12)-H(13)	0.931	1.076	1.088	1.085	1.086	C(5)-C(10)-C(18)	121.14	120.35	119.67	121.78	121.78
C(12)-C(14)	1.338	1.372	1.392	1.379	1.377	C(11)-C(10)-C(18)	117.90	118.60	119.24	117.83	117.93
C(14)-H(15)	0.930	1.076	1.087	1.085	1.086	N(2)-C(11)-C(10)	122.40	122.90	121.84	122.08	121.87
C(14)-C(16)	1.374	1.393	1.403	1.403	1.401	N(2)-C(11)-C(12)	119.41	118.70	119.69	119.26	119.52
C(16)-H(17)	0.930	1.074	1.086	1.083	1.084	C(10)-C(11)-C(12)	118.18	118.34	118.17	118.65	118.61
C(16)-C(18)	1.356	1.374	1.392	1.381	1.379	C(11)-C(12)-H(13)	119.10	118.69	118.60	118.46	118.50
C(18)-H(19)	0.929	1.073	1.086	1.081	1.082	C(11)-C(12)-C(14)	121.83	121.32	121.50	121.38	121.34
C(20)-C(21)	1.365	1.392	1.406	1.404	1.402	H(13)-C(12)-C(14)	119.08	119.98	119.84	120.16	120.16
C(20)-C(28)	1.358	1.388	1.405	1.402	1.400	C(12)-C(14)-H(15)	119.59	119.22	119.43	119.41	119.35
C(21)-H(22)	0.929	1.073	1.087	1.083	1.084	C(12)-C(14)-C(16)	120.71	120.83	120.29	120.58	120.65
C(21)-C(23)	1.361	1.381	1.396	1.389	1.387	H(15)-C(14)-C(16)	119.70	119.95	120.27	120.01	120.00
C(23)-H(24)	0.929	1.076	1.088	1.086	1.088	C(14)-C(16)-H(17)	120.32	120.93	120.62	120.63	120.66
C(23)-N(25)	1.313	1.322	1.347	1.339	1.336	C(14)-C(16)-C(18)	119.23	118.37	118.99	118.90	118.84
N(25)-C(26)	1.306	1.317	1.345	1.335	1.332	H(17)-C(16)-C(18)	120.44	120.70	120.36	120.47	120.50
C(26)-H(27)	0.930	1.076	1.088	1.086	1.088	C(10)-C(18)-C(16)	122.14	122.50	121.61	122.64	122.63
C(26)-C(28)	1.371	1.386	1.398	1.392	1.390	C(10)-C(18)-H(19)	118.90	119.17	119.13	119.36	119.32
C(28)-H(29)	0.931	1.075	1.087	1.084	1.085	C(16)-C(18)-H(19)	118.96	118.31	119.26	117.99	118.05
						C(8)-C(20)-C(21)	123.97	123.68	123.23	124.19	124.11
						C(8)-C(20)-C(28)	119.39	119.27	119.92	119.28	119.34
						C(21)-C(20)-C(28)	116.64	117.05	116.85	116.53	116.55
						C(20)-C(21)-H(22)	120.45	121.61	121.00	121.31	121.32
						C(20)-C(21)-C(23)	119.22	118.92	119.25	119.35	119.29
						H(22)-C(21)-C(23)	120.33	119.46	119.74	119.33	119.38
						C(21)-C(23)-H(24)	117.64	119.93	120.08	120.04	119.99
						C(21)-C(23)-N(25)	124.69	123.88	124.13	123.99	124.08
						H(24)-C(23)-N(25)	117.67	116.18	115.79	115.97	115.92
						C(23)-N(25)-C(26)	115.68	117.35	116.39	116.81	116.73
						N(25)-C(26)-H(27)	118.04	116.41	115.90	116.19	116.14
						N(25)-C(26)-C(28)	123.84	123.59	123.90	123.65	123.75
						H(27)-C(26)-C(28)	118.12	120.00	120.19	120.16	120.11
						C(20)-C(28)-C(26)	119.91	119.20	119.46	119.66	119.59
						C(20)-C(28)-H(29)	120.08	120.86	120.35	120.30	120.30
						C(26)-C(28)-H(29)	120.00	119.94	120.19	120.04	120.11

[a] Geometric parameters determined with X-ray diffraction method from Ref. [22].

and the calculated ones belong to the gas phase. Secondly, calculus has been done for an isolated molecule in gas phase and the experimental values include intermolecular interactions. That is why a correction of the calculated frequencies through a scale factor for all methods is needed [28] [18]; 0.899748 HF/6-311G (d, p); 0.956853 MP2/6-311G (d, p) 0.960461 B3LYP/6−311++G (d, p); 0.957562 B3PW91/6−311++G (d, p).

The specific allocation for each frequency was performed according to the potential energy distribution (PED) (Table 4), using the VEDA software [27]. The PED for the scaled vibrational frequencies, at level DFT/B3LYP, was deeply analyzed since they were the closest to the experimental observed data.

4.2.1. N−H vibrations

The phenylamine (aromatic primary amine) has two sharp N−H bands, the asymmetrical N−H stretch showing such bands in the $3420 \ cm^{-1}$ — $3500 \ cm^{-1}$ range and the symmetrical N−H stretch showing bands at $3340 \ cm^{-1}$ — $3420 \ cm^{-1}$ [29]. These vibrations were calculated at $3526 \ cm^{-1}$ and $3432 \ cm^{-1}$ for 2-

aminoterephthalic in previous works [30]. In 2-aminochalcone these bands were observed at $3392 \ cm^{-1}$ and $3263 \ cm^{-1}$, and calculated at $3541 \ cm^{-1}$ and $3432 \ cm^{-1}$ (HF); $3545 \ cm^{-1}$ and $3417 \ cm^{-1}$ (MP2); $3555 \ cm^{-1}$ and $3372 \ cm^{-1}$ (B3LYP); $3563 \ cm^{-1}$ and $3355 \ cm^{-1}$ (B3PW91).

The N−H bending vibration of aromatic primary amines gives a strong intensity band between $1638 \ cm^{-1}$ and $1575 \ cm^{-1}$ [31]. This vibration has been calculated before at $1596 \ cm^{-1}$ for nicotinamide N-oxide in previous studies [32]. For 2-aminochalcone it was observed at $1623 \ cm^{-1}$ and calculated at $1559 \ cm^{-1}$ (HF); $1594 \ cm^{-1}$ (MP2); $1568 \ cm^{-1}$ (B3LYP); $1544 \ cm^{-1}$ (B3PW91).

The N−H wagging band for aromatic primary amines gives a band between $650 \ cm^{-1}$ to $900 \ cm^{-1}$ [33]. This vibration was calculated at $575 \ cm^{-1}$ (HF); $612 \ cm^{-1}$ (MP2); $654 \ cm^{-1}$ (B3LYP); $667 \ cm^{-1}$ (B3PW91).

4.2.2. C−H vibrations

The C−H vibration (stretching) bands of aromatic compounds appear in the $3100 \ cm^{-1}$ — $3000 \ cm^{-1}$ range and exhibits weak to

Table 2
Selected dihedral angles (°) for 2-aminochalcone molecule computed at HF, MP2, B3LYP, and B3PW91 with 6−311++G (d,p) basis set.

Dihedral angles (°)	Exp[a]	Ab initio		DFT	
		HF	MP2	B3LYP	B3PW91
H(3)-N(2)-C(11)-C(10)	3.532	21.133	27.621	5.947	5.306
H(3)-N(2)-C(11)-C(12)	−177.17	−161.679	−158.798	−174.901	−175.452
H(4)-N(2)-C(11)-C(10)	−177.65	166.713	165.091	176.376	177.226
H(4)-N(2)-C(11)-C(12)	1.651	−16.100	−21.327	−4.472	−3.532
O(1)-C(5)-C(6)-H(7)	−179.12	164.272	160.181	174.352	173.879
O(1)-C(5)-C(6)-C(8)	0.82	−14.823	−18.107	−4.410	−4.752
C(10)-C(5)-C(6)-H(7)	1.851	−15.093	−18.597	−4.963	−5.354
C(10)-C(5)-C(6)-C(8)	−178.21	165.812	163.115	176.276	176.015
O(1)-C(5)-C(10)-C(11)	−9.50	−18.498	−19.814	−5.471	−5.729
O(1)-C(5)-C(10)-C(18)	169.06	159.576	155.995	173.883	173.686
C(6)-C(5)-C(10)-C(11)	169.49	160.850	158.937	173.823	173.480
C(6)-C(5)-C(10)-C(18)	−11.95	−21.076	−25.254	−6.824	−7.105
C(5)-C(6)-C(8)-C(20)	−178.49	179.204	178.317	179.104	179.040
C(6)-C(8)-C(20)-C(21)	2.60	−16.968	22.190	0.647	0.657
C(6)-C(8)-C(20)-C(28)	−177.31	163.357	−157.996	−179.301	−179.284
H(9)-C(8)-C(20)-C(28)	2.66	−15.576	19.502	0.443	0.453
C(5)-C(10)-C(11)-N(2)	−0.69	−3.024	−5.435	−0.370	−0.018
N(2)-C(11)-C(12)-H(13)	0.03	1.450	4.331	0.280	0.109
C(8)-C(20)-C(21)-H(22)	−179.88	179.593	−178.758	−179.945	−179.937
C(28)-C(20)-C(21)-C(23)	0.03	−0.726	1.422	0.005	0.005

[a] Geometric parameters determined with X-ray diffraction method from Ref. [22].

moderate intensities [34], so making them easy to differentiate from those produced by aliphatic C−H groups which appear below 3000 cm^{-1}. The asymmetrical C−H stretching vibration of the phenylamine ring was experimentally observed at 3139 cm^{-1} and was calculated at 3026 cm^{-1} (HF); 3081 cm^{-1} (MP2); 3031 cm^{-1} (B3LYP); 3065 cm^{-1} (B3PW91). The symmetric C−H stretching vibration was experimentally observed at 3077 cm^{-1}, and calculated at 3011 cm^{-1} (HF); 3095 cm^{-1} (MP2); 3049 cm^{-1} (B3LYP); 3051 cm^{-1} (B3PW91). The symmetric C−H stretching vibration of pyridine ring was observed at 3031 cm^{-1} and calculated at 3013 cm^{-1} (HF); 3077 cm^{-1} (MP2); 3054 cm^{-1} (B3LYP); 3027 cm^{-1} (B3PW91).

The C−H bending bands of aromatic compounds appear in the regions 1300 cm^{-1} and 1000 cm^{-1} (in-plane bending) [35]. This vibration of phenylamine ring was experimentally observed at 1155 cm^{-1} and was calculated at 1139 cm^{-1} (HF); 1135 cm^{-1} (MP2); 1143 cm^{-1} (B3LYP); 1131 cm^{-1} (B3PW91). The C−H bending vibration of pyridine ring was experimentally observed at 1080 cm^{-1} and calculated 1008 cm^{-1} (HF); 1039 cm^{-1} (MP2); 1068 cm^{-1} (B3LYP); 1065 cm^{-1} (B3PW91).

The aromatic rings substitution patterns can be identified by the C−H out of plane bending that leads to bands between 900 cm^{-1} and 675 cm^{-1} [35,36]. The characteristic vibrations of the ortho substituted aromatic rings were observed at 760 cm^{-1} and 732 cm^{-1}. These vibrations were calculated at 751 cm^{-1} and 729 cm^{-1} (HF); 760 cm^{-1} and 714 cm^{-1} (MP2); 751 cm^{-1} and 715 cm^{-1} (B3LYP); 761 cm^{-1} and 721 cm^{-1} (B3PW91).

4.2.3. C−C vibrations

The C−C stretching vibrations in the aromatic ring are very important to characterize chalcones. Sathyanarayana, 2004 [37], found that these vibrations give bands between 1430 cm^{-1} and 1650 cm^{-1}. For pyridine ring, C=C vibration was observed at 1546 cm^{-1} and calculated at 1560 cm^{-1} (HF); 1521 cm^{-1} (MP2); 1565 cm^{-1} (B3LYP); 1575 cm^{-1} (B3PW91). For phenylamine ring, asymmetric and symmetric C=C bond stretching vibrations were observed at 1481 cm^{-1} and 1415 cm^{-1}, respectively, and calculated at 1474 cm^{-1} and 1432 cm^{-1} (HF); 1419 cm^{-1} and 1401 cm^{-1} (MP2); 1451 cm^{-1} and 1412 cm^{-1} (B3LYP); 1447 cm^{-1} and 1412 cm^{-1} (B3PW91).

Deformation vibration of the pyridinic ring hints bands from 1100 cm^{-1} and 950 cm^{-1} [31]. In this work, the deformation vibration of aromatic ring was observed at 981 cm^{-1} and calculated at 978 cm^{-1} (HF); 962 cm^{-1} (MP2); 968 cm^{-1} (B3LYP); 968 cm^{-1} (B3PW91).

4.2.4. C=O vibrations

The C=O stretching vibration hints bands in the region of 1740 cm^{-1} and 1660 cm^{-1} [38]. In this work a strong band was observed at 1651 cm^{-1} and assigned to the C=O stretching vibration, which appears at a frequency slightly lower than the expected since it is forming a α, β-unsaturated system that generates an electron delocalization in the C=O bond. This stretching vibration was calculated at 1710 cm^{-1} (HF); 1626 cm^{-1} (MP2); 1630 cm^{-1} (B3LYP); 1638 cm^{-1} (B3PW91), which was found consistent with some related work [39].

The C=O bending vibration results in bands in the region of 700 cm^{-1} and 600 cm^{-1} [33]. It was observed at 650 cm^{-1} and calculated at 650 cm^{-1} (HF); 685 cm^{-1} (MP2); 653 cm^{-1} (B3LYP); 665 cm^{-1} (B3PW91).

4.2.5. C−N vibrations

The pyridine type compounds and their derivatives show strong bands in the region of 1600 cm^{-1} to 1430 cm^{-1} due to the C=N stretching vibration of the pyridine ring [40]. For 2-aminochalcone a strong band was observed at 1585 cm^{-1} and assigned to the C=N stretching vibration. This was calculated at 1570 cm^{-1} (HF); 1564 cm^{-1} (MP2); 1565 cm^{-1} (B3LYP); 1535 cm^{-1} (B3PW91).

Aromatic amines show C−N stretching vibration bands between 1382 cm^{-1} and 1266 cm^{-1} [41]. In the phenylamine ring such band was observed at 1265 cm^{-1} and was calculated at 1266 cm^{-1} (HF); 1283 cm^{-1} (MP2); 1240 cm^{-1} (B3LYP); 1296 cm^{-1} (B3PW91).

4.3. NMR analysis

Chemical shifts of ^{1}H and ^{13}C NMR were calculated with ab initio and DFT by GIAO method [42,43], from the optimized geometries, with tetramethylsilane (TMS) as standard and DMSO as solvent with CPCM model [44]. Experimental ^{1}H and ^{13}C NMR spectra are shown in Figs. 3 and 4. The experimental chemical shifts of ^{1}H and

Table 3
Vibrational assignments of fundamental observed frequencies and calculated frequencies of 2-aminochalcone with ab initio and DFT.

Modes	Observed frequencies (cm^{-1}) FT-IR (cm^{-1})	Calculated with 6−311++G(d, p) basis set				Characterization of normal modes with PED(%)		
		DFT		Ab initio				
		B3LYP	B3PW91	HF	MP2			
1	3392	3555	3563	3541	3545	s1 (97)		
2	3263	3372	3355	3432	3417	s2 (97)		
3		3098	3093	3041	3095	s6 (88)		
4		3078	3077	3026	3088	s8 (84)		
5	3139	3065	3066	3021	3081	s3 (79)		
6		3063	3064	3013	3078	s11 (10)	s12 (77)	
7	3077	3054	3054	3011	3076	s9 (78)		
8		3049	3051	3003	3070	s5 (11)	s7 (79)	
9		3032	3033	2999	3059	s11 (79)	s12 (11)	
10	3031	3032	3029	2992	3058	s10 (86)		
11		3028	3027	2989	3054	s5 (78)	s7 (11)	
12		3026	3024	2983	3045	s4 (99)		
13	1651	1630	1638	1710	1626	s13 (65)		
14	1623	1589	1599	1652	1594	s23 (48)	s32 (13)	
15		1568	1577	1620	1585	s27 (59)	s33 (13)	
16		1566	1576	1610	1564	s26 (47)		
17		1542	1543	1601	1563	s21 (28)	s32 (14)	
18	1585	1523	1534	1570	1535	s21 (20)	s32 (32)	
19	1546	1512	1515	1560	1521	s22 (69)		
20	1481	1463	1462	1495	1458	s37 (44)	s52 (24)	
21		1451	1447	1475	1452	s39 (56)	s48 (11)	
22	1440	1413	1412	1432	1419	s15 (28)	s38 (40)	
23		1386	1383	1400	1402	s24 (69)		
24	1415	1328	1342	1329	1387	s18 (47)	s42 (30)	
25		1314	1311	1318	1331	s17 (63)		
26	1346	1309	1299	1296	1305	s34 (52)		
27		1296	1296	1284	1287	s14 (10)	s34 (11)	
28	1295	1275	1273	1266	1283	s25 (22)	s38 (27)	
29		1240	1247	1218	1266	s33 (44)		
30	1265	1227	1237	1207	1241	s25 (32)	s36 (15)	
31		1198	1197	1189	1204	s19 (42)	s26 (10)	
32	1214	1181	1187	1179	1192	s26 (13)	s41 (35)	s41 (16)
33		1176	1170	1139	1171	s40 (62)		
34	1155	1143	1136	1105	1135	s23 (11)	s35 (67)	
35		1135	1131	1101	1128	s15 (12)	s36 (56)	
36		1068	1065	1058	1058	s18 (30)	s42 (42)	s39 (14)
37		1047	1046	1046	1050	s21 (15)	s31 (31)	
38	1080	1037	1036	1044	1039	s20 (15)	s39 (11)	
39		999	998	1008	1015	s16 (48)	s31 (11)	
40	1025	982	979	1007	988	s28 (42)	s55 (17)	
41		978	976	1000	962	s20 (58)	s48 (16)	
42		968	968	995	957	s59 (81)		
43	1002	959	956	983	905	s65 (74)	s72 (12)	s48 (50)
44		946	941	978	887	s66 (84)	s37 (12)	
45	981	937	933	976	876	s60 (79)		
46	890	911	906	972	869	s29 (49)		
47		872	870	909	859	s62 (76)		
48		869	865	876	834	s58 (51)	s64 (11)	
49		839	836	868	820	s64 (58)	s65 (13)	
50	842	824	823	850	816	s28 (10)	s52 (16)	
51		821	816	821	791	s63 (82)		
52	815	797	794	817	760	s67 (37)		
53		760	761	768	754	s67 (47)	s79 (10)	
54	760	751	749	757	714	s61 (73)		
55	748	724	722	752	685	s58 (11)	s79 (45)	
56	732	715	713	730	649	s51 (46)		
57		666	665	684	646	s50 (83)		
58		656	651	658	622	s71 (69)		
59	650	653	650	650	612	s74 (57)		
60	576	628	639	561	569	s47 (14)	s75 (45)	
61		562	557	551	546	s49 (53)		
62		547	543	539	535	s45 (17)	s47 (42)	
63		517	514	516	494	s53 (48)		
64		500	495	508	471	s80 (65)		
65	501	494	491	484	457	s56 (51)		
66		426	422	436	432	s57 (68)		
67		420	414	416	401	s30 (65)	s75 (11)	
68		399	398	392	397	s73 (31)		
69		369	364	388	373	s45 (15)	s73 (27)	
70		334	330	383	350	s64 (12)	s72 (75)	
71		263	263	314	300	s43 (42)	s46 (17)	

Table 3 (continued)

Modes	Observed frequencies (cm^{-1})	Calculated with 6−311++G(d, p) basis set				Characterization of normal modes with PED(%)	
		DFT		Ab initio			
	FT-IR (cm^{-1})	B3LYP	B3PW91	HF	MP2		
72		255	252	269	249	s44 (11)	s77 (57)
73		231	230	236	234	s44 (16)	s70 (21)
74		205	204	208	199	s44 (12)	s70 (33)
75		188	187	190	184	s46 (11)	s55 (25)
76		117	113	129	136	s44 (31)	s69 (42)
77		99	98	98	111	s70 (12)	s76 (55)
78		79	77	76	77	s81 (72)	
79		57	54	53	46	s54 (68)	s73 (10)
80		27	27	30	31	s69 (13)	s78 (60)
81		14	12	17	20	s68 (84)	

^{13}C NMR were assigned according to the reported in literature [45,46]. Compound 2-aminochalcone experimental and calculated chemical shifts are presented in Table 5.

In the ^{1}H NMR spectrum chemical shifts between 8.64 ppm and 6.59 ppm were observed, while the calculated were obtained between 8.84 ppm and 3.94 ppm (HF); 8.93 ppm and 6.80 ppm (MP2); 9.18 ppm and 5.02 ppm (B3LYP); 9.24 ppm and 4.99 ppm (B3PW91). Atoms from (H-13), (H −15), (H −17), (H-19) presented aromatic protons characteristically chemical shifts. It was observed that the major deviation in the calculated chemical shift regarding experimental ones (δ_{Exp}-δ_{Theo}) was 3.54 ppm (H-4) with HF. Differences at DFT levels are 2.46 ppm (H-4) with for B3LYP and 2.49 ppm (H-4) B3PW91. They may be due to overestimated paramagnetic contribution in the DFT calculations [47], this is consistent since this deviation occurs for protons of NH$_2$ group, which seems to increase their electron density by the influence of the aromatic ring, and thus all displacements occur at high field likewise, minor deviations were obtained at 0.09 ppm (H-13) with HF, 0.02 ppm (H −13) with MP2, 0.03 ppm (H-29) with B3LYP and 0.02 ppm (H-29) with B3PW91.

In the ^{13}C NMR spectrum chemical shifts between 190 ppm and 115 ppm were observed, finding aromatic ring signals from 150 ppm to 100 ppm [48,49]. In the same way, the calculated chemical shifts were observed between 196 ppm and 116 ppm (HF), 207 ppm and 123 ppm (MP2), 195 ppm and 120 ppm (B3LYP), 193 ppm and 119 ppm (B3PW91). It was noted that deviations of the calculated chemical shifts regarding the experimental ones (δ_{Exp}-δ_{Theo}) were 22 ppm (C-11) with HF, 28 ppm (C-11) with MP2, 20 ppm (C-11) with B3LYP, and 17 ppm (C-11) with B3PW91. Minor deviations were 0.89 ppm (C-12) with HF; 6 ppm (C-20) with MP2, 2 ppm (C-6) with B3LYP, 1.54 ppm (C-6) with B3PW91. In general, calculations at DFT/6-311G++(d,p) level represent a better approximation to the experimentally observed data.

4.4. HOMO and LUMO analysis

Frontier molecular orbitals play a key role in the study of the electrical and optical properties. Both, the highest occupied molecular orbital (HOMO) and the lowest unoccupied molecular orbital (LUMO), could determine the way in which the molecule interacts with other species [50]. The HOMO represent the ability to donate an electron, and the LUMO of accepting an electron [51]. The
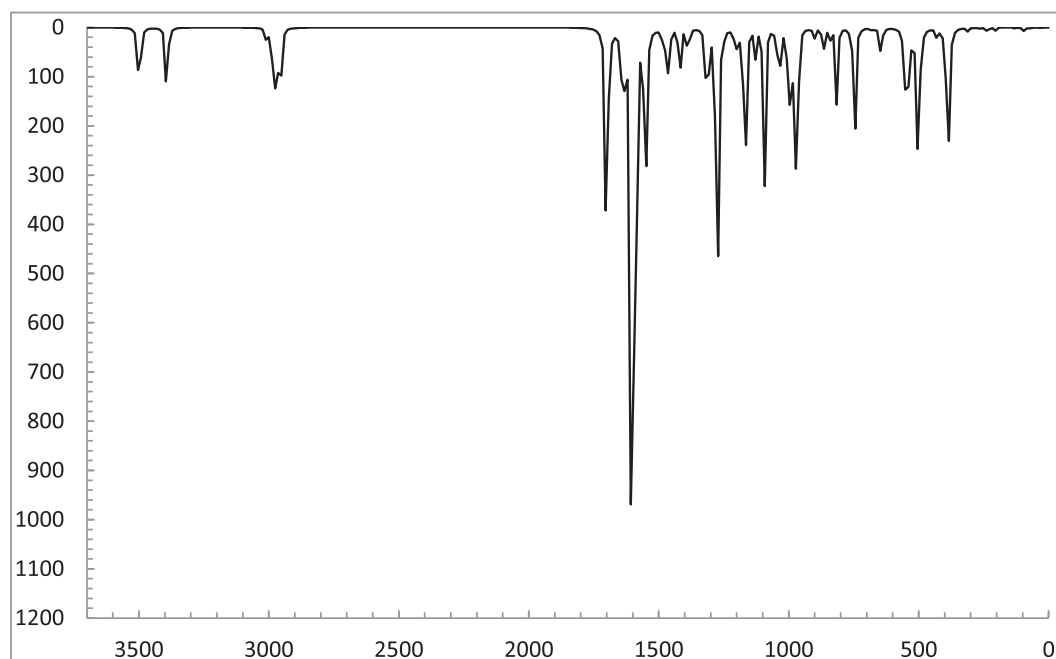
Fig. 6. Calculated FT-IR spectrum of 2-aminochalcone at the HF/6-311G (d, p) level.
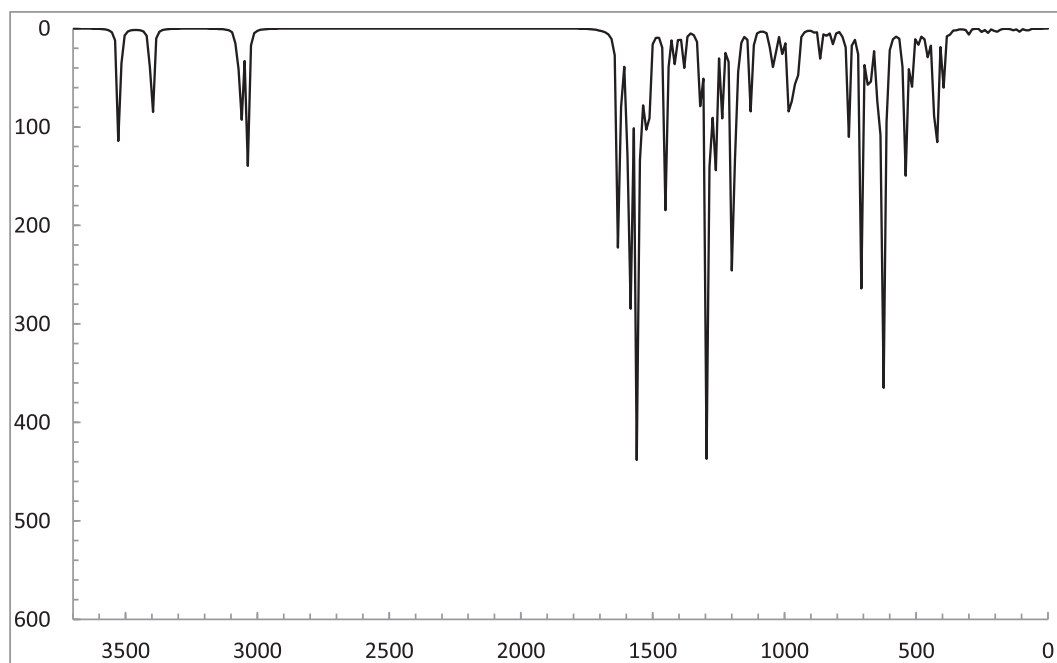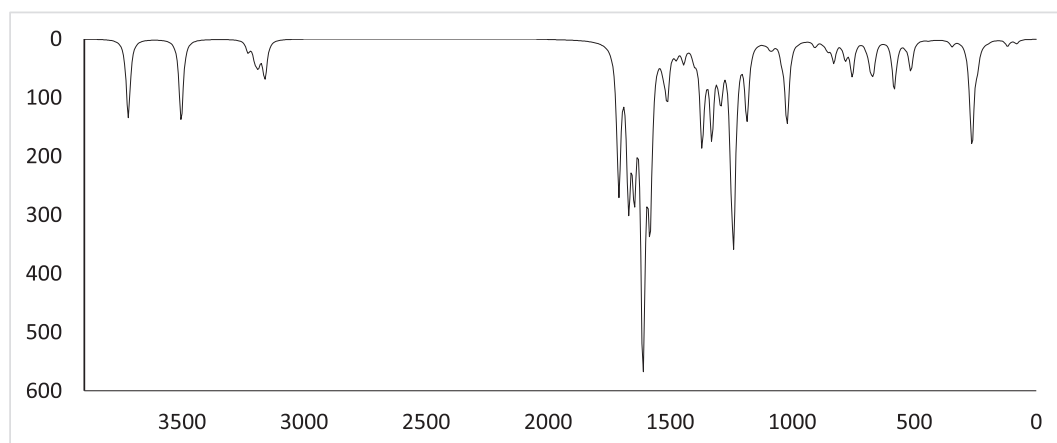
Fig. 7. Calculated FT-IR spectrum of 2-aminochalcone at the MP2/6-311G (d, p) level.
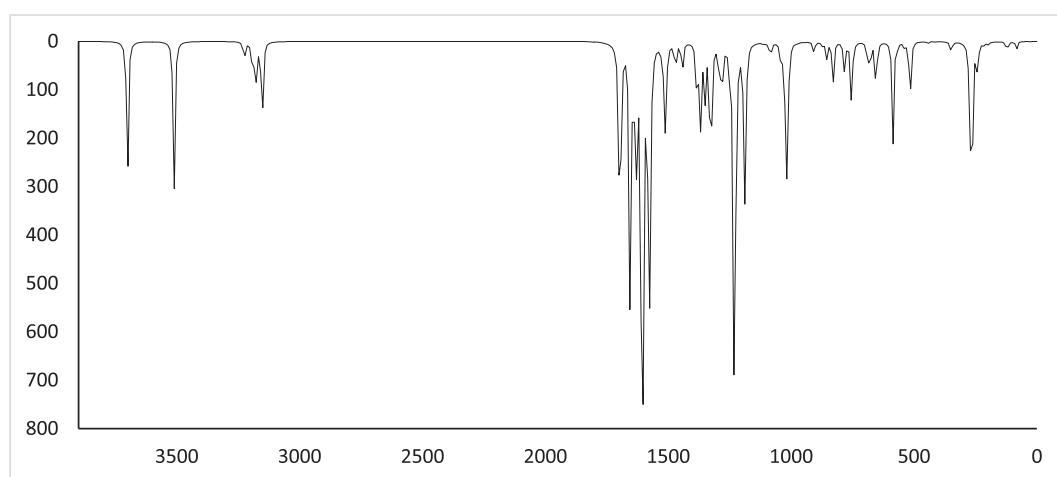
Fig. 8. Calculated FT-IR spectrum of 2-aminochalcone at the B3LYP/6−311++G (d, p) level.

Fig. 9. Calculated FT-IR spectrum of 2-aminochalcone at the B3PW91/6−311++G (d, p) level.

Table 4
Definition of normal modes of vibration (s) obtained with PED. a). Stretching. b). In-plane bending and c). Torsion and Out-of-plane bending.

a). Stretching (υ)

Mode			Atoms	Mode			Atoms	Mode			Atoms
s 1	1	υ	N(2)-H(3)	**s 14**	1	υ	C(5)-C(10)	**s 21**	−1	υ	C(11)-C(12)
	−1	υ	N(2)-H(4)		1	υ	C(8)-C(20)		1	υ	C(14)-C(16)
s 2	1	υ	N(2)-H(3)		1	υ	C(10)-C(18)		−1	υ	C(21)-C(23)
	1	υ	N(2)-H(4)		−1	υ	N(25)-C(23)	**s 22**	1	υ	C(20)-C(28)
s 3	1	υ	C(21)-H(22)	**s 15**	1	υ	C(10)-C(18)		1	υ	N(25)-C(23)
s 4	1	υ	C(8)-H(6)		−1	υ	C(12)-C(14)	**s 23**	1	υ	C(11)-C(12)
s 5	1	υ	C(12)-H(13)		1	υ	C(16)-C(18)		−1	υ	C(12)-C(14)
s 6	1	υ	C(16)-H(17)		−1	υ	N(25)-C(26)	**s 24**	−1	υ	C(10)-C(18)
s 7	1	υ	C(14)-H(15)		−1	υ	N(25)-C(23)		−1	υ	C(11)-C(12)
	−1	υ	C(16)-H(17)	**s 16**	1	υ	C(14)-C(16)		1	υ	C(12)-C(14)
	1	υ	C(16)-H(19)		1	υ	C(12)-C(14)		1	υ	C(16)-C(18)
s 8	1	υ	C(6)-H(7)	**s 17**	1	υ	C(20)-C(28)	**s 25**	1	υ	N(2)-C(11)
	−1	υ	C(16)-H(17)		−1	υ	N(25)-C(23)		−1	υ	C(10)-C(18)
	1	υ	C(16)-H(19)		1	υ	N(25)-C(26)	**s 26**	−1	υ	C(21)-C(23)
	1	υ	C(21)-H(22)	**s 18**	1	υ	C(21)-C(23)		−1	υ	C(26)-C(28)
s 9	1	υ	C(6)-H(7)		−1	υ	C(26)-C(28)		1	υ	N(25)-C(23)
	1	υ	C(14)-H(15)	**s 19**	−1	υ	C(5)-C(10)		1	υ	N(25)-C(26)
s 10	1	υ	C(23)-H(24)		1	υ	C(6)-C(8)	**s 27**	1	υ	C(6)-C(8)
	−1	υ	C(26)-H(27)		1	υ	C(8)-C(20)		1	υ	O(1)-C(5)
s 11	1	υ	C(23)-H(24)		−1	υ	C(21)-C(23)	**s 28**	1	υ	C(5)-C(6)
	1	υ	C(26)-H(27)		−1	υ	C(26)-C(28)		−1	υ	C(11)-C(12)
s 12	1	υ	C(28)-H(29)	**s 20**	1	υ	N(25)-C(26)		1	υ	O(1)-C(5)
s 13	1	υ	O(1)-C(5)		1	υ	N(25)-C(23)				
					1	υ	C(26)-C(28)				

b). In-plane bending (δ)

Mode			Atoms	Mode			Atom
s 29	−1	δ	C(5)-C(6)-C(8)	**s 31**	1	δ	H(3)-N(2)-C(11)
	1	δ	C(23)-N(25)-C(26)		−1	δ	C(11)-C(12)-C(14)
	−1	δ	C(6)-C(8)-C(20)	**s 32**	1	δ	H(3)-N(2)-H(4)
	1	δ	C(20)-C(28)-C(26)		−1	δ	C(14)-C(16)-C(18)
s 30	−1	δ	C(12)-C(11)-N(2)	**s 33**	1	δ	H(7)-C(6)-C(8)
	1	δ	C(11)-C(12)-C(14)		−1	δ	H(9)-C(8)-C(20)
s 34	1	δ	H(9)-C(8)-C(20)	**s 46**	−1	δ	C(5)-C(6)-C(8)
	1	δ	H(24)-C(23)-N(25)		−1	δ	C(6)-C(8)-C(20)
	−1	δ	H(29)-C(28)-C(26)		1	δ	C(10)-C(18)-C(16)
s 35	−1	δ	H(15)-C(14)-C(16)		−1	δ	C(11)-C(12)-C(14)
	1	δ	H(13)-C(12)-C(14)		−1	δ	C(20)-C(28)-C(26)
	1	δ	H(17)-C(16)-C(18)		1	δ	C(21)-C(23)-N(25)
s 36	1	δ	H(17)-C(16)-C(18)	**s 47**	1	δ	C(11)-C(12)-C(14)
	1	δ	H(19)-C(18)-C(16)		−1	δ	C(14)-C(16)-C(18)
s 37	1	δ	H(19)-C(18)-C(16)		1	δ	C(20)-C(28)-C(26)
	1	δ	H(13)-C(12)-C(14)		1	δ	C(28)-C(26)-N(25)
s 38	1	δ	H(15)-C(14)-C(16)	**s 48**	1	δ	C(21)-C(23)-N(25)
	1	δ	H(17)-C(16)-C(18)		1	δ	C(23)-N(25)-C(26)
s 39	1	δ	H(24)-C(23)-N(25)		1	δ	C(28)-C(26)-N(25)
	1	δ	H(27)-C(26)-N(25)	**s 49**	1	δ	C(20)-C(28)-C(26)
s 40	1	δ	H(22)-C(21)-C(23)		1	δ	C(28)-C(26)-N(25)
	1	δ	H(29)-C(28)-C(26)	**s 50**	1	δ	C(21)-C(23)-N(25)
	1	δ	H(9)-C(8)-C(20)		−1	δ	C(28)-C(26)-N(25)
	1	δ	H(7)-C(6)-C(8)	**s 51**	1	δ	C(12)-C(14)-C(16)
	−1	δ	H(27)-C(26)-N(25)		1	δ	C(14)-C(16)-C(18)
s 41	1	δ	H(7)-C(6)-C(8)	**s 52**	1	δ	C(11)-C(12)-C(14)
	−1	δ	H(22)-C(21)-C(23)		1	δ	C(12)-C(14)-C(16)
	1	δ	H(27)-C(26)-N(25)	**s 53**	1	δ	C(8)-C(20)-C(28)
	−1	δ	H(29)-C(28)-C(26)		1	δ	C(6)-C(8)-C(20)
s 42	1	δ	H(22)-C(21)-C(23)		1	δ	C(5)-C(10)-C(18)
	−1	δ	H(29)-C(28)-C(26)		1	δ	C(6)-C(5)-O(1)
	−1	δ	H(24)-C(23)-N(25)		−1	δ	C(6)-C(5)-C(10)
	1	δ	H(7)-C(6)-C(8)	**s 54**	1	δ	C(6)-C(8)-C(20)
	1	δ	H(9)-C(8)-C(20)		−1	δ	C(5)-C(6)-C(8)
s 43	1	δ	C(5)-C(10)-C(18)		1	δ	C(6)-C(5)-C(10)
	1	δ	C(6)-C(5)-O(1)		1	δ	C(5)-C(6)-C(8)
s 44	1	δ	C(8)-C(20)-C(28)	**s 55**	1	δ	C(6)-C(8)-C(20)
	1	δ	C(6)-C(5)-C(10)		1	δ	C(6)-C(8)-C(20)
	1	δ	C(5)-C(10)-C(18)		1	δ	C(10)-C(18)-C(16)
	1	δ	C(5)-C(6)-C(8)		1	δ	C(20)-C(28)-C(26)
s 45	1	δ	C(6)-C(5)-O(1)		−1	δ	C(21)-C(23)-N(25)
	1	δ	C(11)-C(12)-C(14)				
	1	δ	C(12)-C(14)-C(16)				
	−1	δ	C(14)-C(16)-C(18)				
	1	δ	C(20)-C(28)-C(26)				
	1	δ	C(28)-C(26)-N(25)				

c). Torsion (τ) and Out-of-plane bending (γ)

Mode			Atoms	Mode			Atom
s 56	−1	γ	C(8)-C(21)-C(28)-C(20)	s 70	1	τ	C(5)-C(10)-C(18)-C(16)
	−1	τ	C(5)-C(6)-C(8)-C(20)		1	τ	C(11)-C(12)-C(14)-C(16)
	1	τ	C(23)-N(25)-C(26)-C(28)		1	τ	C(12)-C(14)-C(16)-C(18)
s 57	1	τ	H(4)-N(2)-C(11)-C(10)	s 71	1	τ	H(3)-N(2)-C(11)-C(10)
s 58	1	τ	H(7)-C(6)-C(8)-C(20)		1	τ	C(20)-C(28)-C(26)-N(25)
	1	τ	H(9)-C(8)-C(20)-C(21)		1	τ	C(21)-C(23)-N(25)-C(26)
s 59	1	τ	H(9)-C(8)-C(20)-C(21)	s 72	1	τ	C(21)-C(23)-N(25)-C(26)
	−1	τ	H(7)-C(6)-C(8)-C(20)		1	τ	C(23)-N(25)-C(26)-C(28)
s 60	1	τ	H(15)-C(14)-C(16)-C(18)	s 73	1	τ	C(10)-C(18)-C(16)-C(14)
s 61	1	τ	H(15)-C(14)-C(16)-C(18)		−1	τ	C(11)-C(12)-C(14)-C(16)
	1	τ	H(17)-C(16)-C(18)-C(10)	s 74	1	τ	H(3)-N(2)-C(11)-C(10)
	1	τ	H(13)-C(12)-C(14)-C(16)		−1	τ	C(20)-C(28)-C(26)-N(25)
s 62	1	τ	H(17)-C(16)-C(18)-C(10)	s 75	1	τ	C(11)-C(12)-C(14)-C(16)
	1	τ	H(19)-C(18)-C(16)-C(14)		−1	γ	N(2)-C(10)-C(12)-C(11)
s 63	1	τ	H(13)-C(12)-C(14)-C(16)	s 76	1	τ	C(12)-C(14)-C(16)-C(18)
	1	τ	H(19)-C(18)-C(16)-C(14)		−1	τ	C(6)-C(8)-C(20)-C(21)
s 64	1	τ	H(29)-C(28)-C(26)-N(25)		−1	τ	C(5)-C(10)-C(18)-C(16)
	1	τ	H(22)-C(21)-C(23)-N(25)		−1	τ	C(5)-C(6)-C(8)-C(20)
s 65	1	τ	H(24)-C(23)-N(25)-C(26)		1	τ	C(11)-C(12)-C(14)-C(16)
	1	τ	H(27)-C(26)-N(25)-C(23)	s 77	1	τ	C(5)-C(6)-C(8)-C(20)
s 66	−1	τ	H(29)-C(28)-C(26)-N(25)		1	γ	C(8)-C(21)-C(28)-C(20)
	−1	τ	H(24)-C(23)-N(25)-C(26)		1	τ	C(20)-C(28)-C(26)-N(25)
	1	τ	H(27)-C(26)-N(25)-C(23)		1	τ	C(23)-N(25)-C(26)-C(28)
s 67	−1	τ	H(22)-C(21)-C(23)-N(25)	s 78	1	τ	C(5)-C(6)-C(8)-C(20)
	−1	τ	H(24)-C(23)-N(25)-C(26)		1	τ	C(6)-C(5)-C(10)-C(18)
	1	τ	H(29)-C(28)-C(26)-N(25)	s 79	1	γ	O(1)-C(6)-C(10)-C(5)
s 68	1	τ	C(6)-C(8)-C(20)-C(21)	s 80	1	τ	C(10)-C(18)-C(16)-C(14)
	1	τ	C(8)-C(6)-C(5)-C(10)		1	τ	C(11)-C(12)-C(14)-C(16)
s 69	1	τ	C(5)-C(6)-C(8)-C(20)	s 81	1	γ	N(2)-C(10)-C(12)-C(11)
	−1	τ	C(5)-C(10)-C(18)-C(16)		1	τ	C(5)-C(6)-C(8)-C(20)
	1	τ	C(6)-C(8)-C(20)-C(21)				
	1	τ	C(12)-C(14)-C(16)-C(18)				

difference in the frontier orbital energy allows us to characterize the molecule chemical reactivity and stability. A molecule with a small difference in the frontier orbital energy is generally more reactive [52]. That is, a small HOMO-LUMO gap implies low kinetic stability and high chemical reactivity, because it is energetically favorable to add electrons to a high lying LUMO and to extract electrons from a low-lying HOMO. Among many other uses, the energy difference between the HOMO and LUMO have been used to predict the activity and intramolecular charge transfer in organic molecules with conjugated π bonds [53,54].

Energies gap (HOMO-2 − LUMO+2, HOMO−1 - LUMO+1, and HOMO − LUMO) for 2-aminochalcone were calculated and presented in Table 6. The composition of frontier molecular orbitals is shown in Fig. 10 and the density states diagram is shown in Fig. 11, from them one can see that the HOMO orbitals are partially localized in the phenylamine ring and carbonyl group, while the LUMO orbitals are fully delocalized on the whole molecule. The HOMO and LUMO are qualitatively similar to those obtained by Oumi et al. [55].

The difference in the energy of the frontier orbitals (HOMO −

Table 5
Calculated (δTheo.) and experimental (δExp.) ^{1}H and ^{13}C NMR chemical shifts for the 2-aminochalcone.

| Atom	Exp	Ab initio		DFT	
		HF 6−311++G(d,p)	MP2 6-311G(d,p)	B3LYP 6−311++G(d,p)	B3PW91 6−311++G(d,p)
H(27)	8.64	8.84	8.93	9.18	9.24
H(7)	8.18	7.71	7.74	8.87	8.84
H(19)	8.09	8.25	8.34	8.62	8.61
H(29)	7.80	7.59	7.52	7.77	7.82
H(9)	7.56	8.28	8.47	7.94	8.20
H(4)	7.48	3.94	7.15	5.02	4.99
H(15)	7.30	7.85	7.72	7.64	7.67
H(13)	6.81	6.90	6.83	7.20	7.21
H(17)	6.59	6.71	6.80	6.89	6.95
C(5)	190	196	207	195	193
C(20)	152	153	158	150	148
C(26)	151	159	166	162	161
C(11)	142	164	170	161	159
C(8)	139	149	158	147	147
C(14)	135	148	154	145	144
C(18)	132	144	150	141	139
C(6)	128	130	137	130	130
C(28)	123	129	129	135	134
C(12)	117	118	123	123	122
C(16)	115	116	123	120	119

Table 6
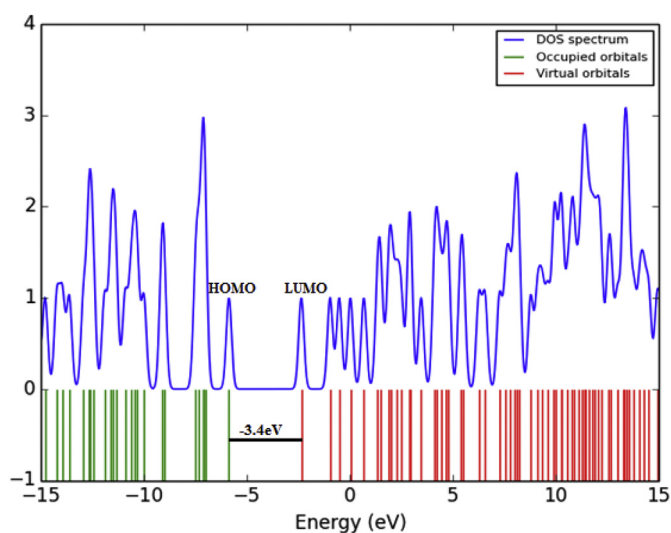Selected HOMO and LUMO energies and energy gap values (eV) of 2-aminochalcone.

Method	Energy (eV)				
Basis set 6−311++G(d,p)	HOMO	LUMO	HOMO−LUMO gap	ΔE[a]	ΔE[b]
B3LYP	−6.0	−2.7	−3.3	−5.8	−6.4
HF	−8.2	0.9	−9.2	−10.5	−10.8
MP2	−8.3	0.8	−9.1	−10.4	−10.8

[a] ΔE(HOMO-1−ELUMO+1) gap (eV).
[b] ΔE(HOMO-2−ELUMO+2) gap (eV).
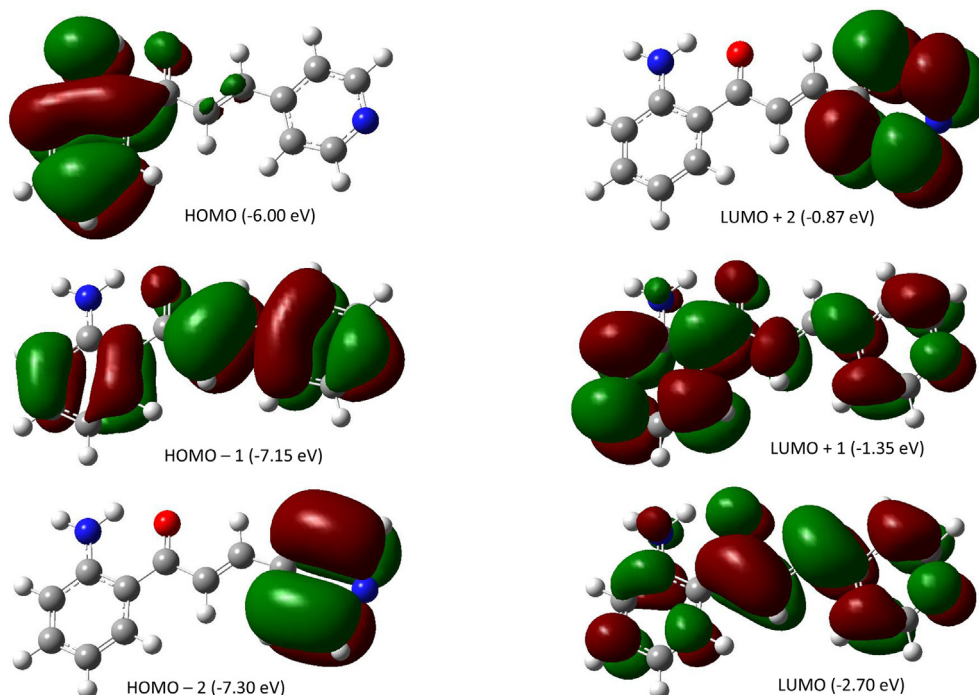
Fig. 10. The atomic orbital composition of the frontier molecular orbital for 2-aminochalnone at the B3LYP/6−311++G (d, p) level.

Fig. 11. Density of states (DOS) diagrams for 2-aminochalcone.

LUMO) allows us to infer that the molecule is reactive to other species to form the activated complex of any potential reaction. It also explains the possible transition involved long-range charge transfer that take place from one phenyl ring to the other within the molecule. The transition from the ground state to the first excited state is mainly described by the excitation of an electron from the HOMO to LUMO [56]. The π nature LUMO is fully delocalized throughout the molecule. In summary, the HOMO-LUMO transition involves a transfer of electron densities to other atoms.

5. Conclusion

(*E*)-1-(2-aminophenyl)-3-(pyridine-4-yl)prop-2-en-1-one was synthesized via Claisen Schmidt condensation and characterized by FT-IR spectroscopy, ^{1}H and ^{13}C NMR, and GC−MS. Calculated geometrical parameters of the 2-aminochalcone correspond with the XRD results reported. The vibrational frequencies observed in the FT-IR spectrum were assigned based on potential energy distribution (PED) and calculi were corroborated by ab initio and DFT level. Considering the fact that the experimental results were performed on solid state (KBr), while calculi takes place for an isolated molecule in the gas phase, the comparative analysis of the experimental and theoretical frequencies of 2−aminochalcone showed

that the calculated frequencies were consistent with experimental results, with DFT method (B3LYP and B3PW91) representing the best approximation to experimental values. ^{1}H and ^{13}C NMR chemical shifts were calculated by the GIAO method and represented a good approximation to the experimentally observed. The energy difference between HOMO-LUMO partly explains the molecule reactivity of and the possible charge transfer interactions taking place on it.

Acknowledgments

References

[1] B.P. Bandgar, S.S. Gawande, R.G. Bodade, J.V. Totre, C.N. Khobragade, Bioorg. Med. Chem. 18 (2010) 1364–1370, http://dx.doi.org/10.1016/j.bmc.2009.11.066.

[2] S.t. V. Kostanecki, J. Tambor, Chem. Ber. 32 (1899) 1921–1926, http://dx.doi.org/10.1002/cber.18990320293.

[3] O. Prakash, A. Kumar, A. Sadana, R. Prakash, S.P. Singh, R.M. Claramunt, D. Sanz, I. Alkorta, J. Elguero, Tetrahedron 61 (2005) 6642–6651, http://dx.doi.org/10.1016/j.tet.2005.03.035.

[4] Y.R. Prasad, A.L. Rao, L. Prasoona, K. Murali, P.R. Kumar, Bioorg. Med. Chem. Lett. 15 (2005) 5030–5034, http://dx.doi.org/10.1016/j.bmcl.2005.08.040.

[5] S. Raghavan, K. Anuradha, Tetrahedron Lett. 43 (2002) 5181–5183, http://dx.doi.org/10.1016/S0040-4039(02)00972-3.

[6] R.B. Kshatriya, Y.I. Shaikh, G.M. Nazeruddin, Orient. J. Chem. 29 (4) (2013) 1475–1487, http://dx.doi.org/10.13005/ojc/290425.

[7] S. Murakami, M. Muramatsu, H. Aihara, S. Otomo, Biochem. Pharmacol. 42 (1991) 1447–1451, http://dx.doi.org/10.1016/0006-2952(91)90458-H.

[8] L. Mathiesen, K.E. Malterud, R.B. Sund, Planta Med. 61 (6) (1995) 515–518, http://dx.doi.org/10.1055/s-2006-959360.

[9] N. Singh, J. Pandey, A. Yadav, V. Chaturvedi, S. Bhatnagar, A.N. Gaikwad, S. Kumar-Sinha, A. Kumar, P.K. Shukla, R.P. Tripathi, Eur. J. Med. Chem. 44 (2008) 1705–1709, http://dx.doi.org/10.1016/j.ejmech.2008.09.026.

[10] S.N. López, M.V. Castelli, S.A. Zacchino, J.N. Domínguez, G. Lobo, J. Charris-Charris, J.C. Cortés, J.C. Ribas, C. Devia, A.M. Rodríguez, R.D. Enriz, Bioorg. Med. Chem. 9 (2001) 1999–2013, http://dx.doi.org/10.1016/S0968-0896(01)00116-X.

[11] B.K. Sarojini, B. Narayana, B.V. Ashalatha, J. Indira, K.G. Lobo, J. Cryst. Grow. 295 (2006) 54–59, http://dx.doi.org/10.1016/j.jcrysgro.2006.07.013.

[12] H.J. Ravindra, K. Chandrashekaran, W.T.A. Harrison, S.M. Dharmaprakash, Appl. Phys. B 94 (2009) 503–511, http://dx.doi.org/10.1007/s00340-008-3248-3.

[13] P. Poornesh, S. Shettigar, G. Umesh, K.B. Manjunatha, K.P. Kamath, B.K. Sarojini, B. Narayana, Opt. Mater. 31 (2009) 854–859, http://dx.doi.org/10.1016/j.optmat.2008.09.007.

[14] R. Prajapati, S. Kumar-Dubey, R. Gaur, R. Kumar-Koiri, B. Kumar-Maurya, S. Kumar-Trigun, L. Mishra, Polyhedron 29 (2010) 1055–1061, http://dx.doi.org/10.1016/j.poly.2009.11.012.

[15] C.N. Khobragade, R.G. Bodade, M.S. Shinde, D.R. Jaju, R.B. Bhosle, B.S. Dawane, J. Enzyme Inhib. Med. Chem. 23 (2008) 341–346, http://dx.doi.org/10.1080/14756360701608585.

[16] S. Sagawa, Y. Nihro, H. Ueda, T. Miki, H. Matsumoto, T. Satoh, Biol. Pharm. Bull. 17 (1994) 251–256, http://dx.doi.org/10.1248/bpb.17.251.

[17] O. Nerya, R. Musa, S. Khatib, S. Tamir, J. Vaya, Phytochemistry 65 (2004) 1389–1395, http://dx.doi.org/10.1016/j.phytochem.2004.04.016.

[18] V. Karunakaran, V. Balachandran, J. Mol. Struct. 1053 (2013) 66–78, http://dx.doi.org/10.1016/j.molstruc.2013.08.057.

[19] Y. Xue, Y. Liu, L. An, L. Zhang, Y. Yuan, J. Mou, L. Liu, Y. Zheng, Comp. Theor. Chem. 965 (2011) 146–153, http://dx.doi.org/10.1016/j.comptc.2011.01.042.

[20] Y. Xue, X. Gong, J. Mol. Struct. Theoch 901 (2009) 226–231, http://dx.doi.org/10.1016/j.theochem.2009.01.034.

[21] R. Abonia, D. Insuasty, J. Castillo, B. Insuasty, J. Quiroga, M. Nogueras, J. Cobo, Eur. J. Med. Chem. 57 (2012) 29–40, http://dx.doi.org/10.1016/j.ejmech.2012.08.039.

[22] F. Cuenú, R. Abonía, J. Cobo, C. Glidewell, Acta Cryst. C 66 (2010) o589–o592, http://dx.doi.org/10.1107/S0108270110040825.

[23] C. Lee, W. Yang, R.G. Parr, Phys. Rev. B 37 (1988) 785–789, http://dx.doi.org/10.1103/PhysRevB.37.785.

[24] J.P. Perdew, K. Burke, Y. Wang, Phys. Rev. B 54 (1996) 16533–16539, http://dx.doi.org/10.1103/PhysRevB.54.16533.

[25] M.J. Frisch, G.W. Trucks, H.B. Schlegel, G.E. Scuseria, M.A. Robb, J.R. Cheeseman, G. Scalmani, V. Barone, B. Mennucci, G.A. Petersson, H. Nakatsuji, M. Caricato, X. Li, H.P. Hratchian, A.F. Izmaylov, J. Bloino, G. Zheng, J.L. Sonnenberg, M. Hada, M. Ehara, K. Toyota, R. Fukuda, J. Hasegawa, M. Ishida, T. Nakajima, Y. Honda, O. Kitao, H. Nakai, T. Vreven, J.A. Montgomery Jr., J.E. Peralta, F. Ogliaro, M. Bearpark, J.J. Heyd, E. Brothers, K.N. Kudin, V.N. Staroverov, T. Keith, R. Kobayashi, J. Normand, K. Raghavachari, A. Rendell, J.C. Burant, S.S. Iyengar, J. Tomasi, M. Cossi, N. Rega, J.M. Millam, M. Klene, J.E. Knox, J.B. Cross, V. Bakken, C. Adamo, J. Jaramillo, R. Gomperts, R.E. Stratmann, O. Yazyev, A.J. Austin, R. Cammi, C. Pomelli, J.W. Ochterski, R.L. Martin, K. Morokuma, V.G. Zakrzewski, G.A. Voth, P. Salvador, J.J. Dannenberg, S. Dapprich, A.D. Daniels, O. Farkas, J.B. Foresman, J.V. Ortiz, J. Cioslowski, D.J. Fox, Gaussian 09, Revision D.01, Gaussian, Inc, Wallingford CT, 2013.

[26] A. Frisch, A.B. Neilson, A.J. Holder, GAUSSVIEW User Manual, Gaussian Inc, Pittsburgh,CT, 2009.

[27] a M.H. Jamroz, Vibrational Energy Distribution Analysis VEDA 4, Warsaw, 2004–2010;
b M.H. Jamroz, Spectrochim. Acta Part A 114 (2013) 220–230, http://dx.doi.org/10.1016/j.saa.2013.05.096.

[28] K.K. Irikura, R.D. Johnson III, R.N. Kacker, J. Phys. Chem. A 109 (2005) 8430–8437, http://dx.doi.org/10.1021/jp052793n.

[29] L.J. Bellamy, The Infrared Spectra of Complex Molecules, vol. 2, Chapman and Hall, London, 1980.

[30] M. Karabacak, M. Cinar, Z. Unal, M. Kurt, J. Mol. Struct. 982 (2010) 22–27, http://dx.doi.org/10.1016/j.molstruc.2010.07.033.

[31] D. Lin-Vien, N.B. Colthup, W.G. Fateley, J.G. Grasselli, The Handbook of Infrared and Raman Characteristic Frequencies of Organic Molecules, Academic Press, Boston, MA, 1991.

[32] A. Atac, M. Karabacak, E. Kose, C. Karaca, Spectrochim. Acta, Part A 83 (2011) 250–258, http://dx.doi.org/10.1016/j.saa.2011.08.027.

[33] N.P.G. Roeges, A Guide to the Complex Interpretation of Infrared Spectra of Organic Structures, Wiley, New York, 1994.

[34] J. Coates, in: R.A. Meyers (Ed.), Interpretation of Infrared Spectra: a Practical Approach, John Wiley and Sons Ltd, Chichester, 2000.

[35] B. Stuart, Infrared Spectroscopy: Fundamentals and Applications, John Wiley & Sons, England, 2004.

[36] P.S. Kalsi, Spectroscopy of Organic Compounds, Wiley Eastern Publisher, New Delhi, 1993.

[37] D.N. Sathyanarayana, Vibrational Spectroscopy Theory and Applications, second ed., New Age International (P) Ltd. Publishers, New Delhi, 2004.

[38] J. Mohan, Organic Spectroscopy-principle and Applications, second ed., Narosa Publishing House, New Delhi, 2000.

[39] .N. Udaya Sri, K. Chaitanya, M.V.S. Prasad, V. Veeraiah, A. Veeraiah, Spectrochim. Acta. A 97 (2012) 728–736, http://dx.doi.org/10.1016/j.saa.2012.07.055.

[40] P.S. Kalsi, Spectroscopy of Organic Compounds, Wiley Eastern Limited, New Delhi, 2007.

[41] M. Silverstein, G. Clayton Basseler, C. Moril, Spectrometric Identification of Organic Compounds, Wiley, New York, 1981.

[42] R. Ditchfield, Mol. Phys. 274 (1974) 789–807, http://dx.doi.org/10.1080/00268977400100711.

[43] K. Wolinski, J.F. Hinton, P. Pulay, J. Am. Chem. Soc. 112 (1990) 8251–8260, http://dx.doi.org/10.1021/ja00179a005.

[44] M. Cossi, N. Rega, G. Scalmani, V. Barone, J. Comp. Chem. 24 (2003) 669–681, http://dx.doi.org/10.1002/jcc.10189.

[45] Y.R. Sharma, Elementary Organic Spectroscopy, S. Chand, New Delhi, 2006.

[46] F.L. Tobiason, J.H. Goldstein, Spectrochim. Acta A 23 (1967) 1385–1395, http://dx.doi.org/10.1016/0584-8539(67)80360-X.

[47] S. Muthu, E.E. Porchelvi, Spectrochim. Acta, Part A 116 (2013) 220–235, http://dx.doi.org/10.1016/j.saa.2013.07.016.

[48] K. Pihlaja, E. Kleinpeter, Carbon-13 Chemical Shifts in Structural and Sterochemical Analysis, VCH Publishers, Deerfield Beach, 1994.

[49] H.O. Kalonowski, S. Berger, S. Braun, Carbon-13 NMR Spectroscopy, John Wiley & Sons, Chichester, 1988.

[50] G. Gece, Corros. Sci. 50 (2008) 2981–2992, http://dx.doi.org/10.1016/j.corsci.2008.08.043.

[51] K. Fukui, Science 218 (1982) 747–754, http://dx.doi.org/10.1126/science.218.4574.747.

[52] I. Fleming, Frontier Orbitals and Organic Chemical Reactions, John Wiley and Sons, New York, 1976.

[53] L. Padmaja, C. Ravikumar, D. Sajan, I. Hubert Joe, V.S. Jayakumar, G.R. Pettit, O. Faurskov Nielsen, J. Raman Spectrosc. 40 (2009) 419–428, http://dx.doi.org/10.1002/jrs.2145.

[54] C. Ravikumar, I.H. Joe, V.S. Jayakumar, Chem. Phys. Lett. 460 (2008) 552–558, http://dx.doi.org/10.1016/j.cplett.2008.06.047.

[55] O. Manabu, M. David, H. Martin Gordon, Spectrochim. Acta Part A 55 (1998) 525–537, http://dx.doi.org/10.1016/S1386-1425(98)00260-1.

[56] M. Kurt, P.C. Babu, N. Sundaraganesan, M. Cinar, M. Karabacak, Spectrochim. Acta Part A 79 (2011) 1162–1170, http://dx.doi.org/10.1016/j.saa.2011.04.037.